A strategy to capture and characterize the synaptic transcriptome

Sathyanarayanan V. Puthanveettil[a,b,c,1], Igor Antonov[a], Sergey Kalachikov[d], Priyamvada Rajasethupathy[a], Yun-Beom Choi[a,e], Andrea B. Kohn[f,g], Mathew Citarella[f,g], Fahong Yu[f,g], Kevin A. Karl[b], Maxime Kinet[a], Irina Morozova[d], James J. Russo[d], Jingyue Ju[d], Leonid L. Moroz[f,g], and Eric R. Kandel[a,b,e,h,1]

[a]Department of Neuroscience and [b]Howard Hughes Medical Institute, Columbia University, New York, NY 10027; [c]Department of Neuroscience, The Scripps Research Institute, Jupiter, FL 33458; [d]Department of Chemical Engineering and Columbia Genome Center, Columbia University, New York, NY 10027; [e]Department of Neurology, College of Physicians and Surgeons of Columbia University, New York, NY 10032; [f]Whitney Laboratory for Marine Biosciences and [g]Department of Neuroscience and McKnight Brain Institute, University of Florida, Gainesville, FL 32611; and [h]Kavli Institute for Brain Science, College of Physicians and Surgeons of Columbia University, New York, NY 10032

Contributed by Eric R. Kandel, March 15, 2013 (sent for review September 7, 2012)

Here we describe a strategy designed to identify RNAs that are actively transported to synapses during learning. Our approach is based on the characterization of RNA transport complexes carried by molecular motor kinesin. Using this strategy in *Aplysia*, we have identified 5,657 unique sequences consisting of both coding and noncoding RNAs from the CNS. Several of these RNAs have key roles in the maintenance of synaptic function and growth. One of these RNAs, myosin heavy chain, is critical in presynaptic sensory neurons for the establishment of long-term facilitation, but not for its persistence.

long-term memory storage | RNA transport | local protein synthesis | neurogenomics | cystoskeleton

Despite decades of research on the importance of local translation in learning-related synaptic plasticity and long-term memory storage, we know relatively little about the identity of the "synaptic transcriptome," the various components of the total RNA population that is transported from the cell body, and how this transcriptome becomes localized to and translated at specific synapses (1–12). To develop a general strategy for isolating and characterizing all of the RNAs transported from the cell body to the synapse, we have focused on the RNA transport complexes that interact with the molecular motor kinesin that mediate transport of gene products from the cell body to synapses (13, 14).

Our approach offers four distinct advantages over previously described methods: (*i*) it allows the identification of RNAs based on their association with transport machinery that is destined for synapses; (*ii*) it reflects dynamically regulated RNAs; (*iii*) it allows for identification of the targeted RNAs; and (*iv*) it can be used in different regions of the central nervous system (CNS), thereby facilitating genomic characterization of synaptic transcriptome of the entire CNS or region of the CNS. These advantages should aid the study of stoichiometric changes in localized RNAs and their role of local translation, not only in memory storage, but also in a variety of other physiological conditions, such as development. Using this strategy, we have succeeded in obtaining a comprehensive collection of RNAs targeted to *Aplysia* CNS synapses. We further show that myosin heavy chain mRNA, a cargo of kinesin, is localized to sensory neuron processes and is required specifically for the induction of long-term facilitation (LTF) at sensory and motor neuron synapses.

Results

Strategy for Identifying Synaptically Targeted RNAs: Isolation and Characterization of RNA Transport Complexes. We assumed that successful isolation of the RNA–protein complexes associated with the kinesin transport machinery would help identify the full repertoire of RNAs that are actively transported to synapses. Because the CNS contains both neuronal and nonneuronal cells, this approach will also yield RNAs found in the kinesin complex in nonneuronal cells, such as glia. We first optimized conditions for isolating RNA transport complexes from the CNS of *Aplysia* based on a previously described protocol for preparation of kinesin transport complexes Aplysia Kinesin Heavy Chain 1 (ApKHC1) that contain several synaptic proteins (15). To examine whether the transport complexes prepared from CNS contain RNA cargos (Fig. 1 *A* and *B*), we searched in the complex for the presence of three RNA-binding proteins known to be present at synapses—staufen, fragile X mental retardation protein (FMRP), and cytoplasmic polyadenylation element-binding protein (CPEB)—that have been associated with kinesin in the mouse (14, 16). Western blot analysis of the coimmunoprecipitated Kinesin Heavy Chain (KHC) complex revealed the presence of all three of these RNA-binding proteins (Fig. 1*C*) specifically in the kinesin coimmunoprecipitations (CoIPs), but not in the Aplysia Target of Rapamycin (ApTOR) Ab (used as a nonspecific Ab control) CoIPs. Thus, the kinesin complex immunoprecipitated from CNS contains several RNA-binding proteins and is likely to contain RNAs destined for synaptic sites.

We next prepared RNAs from the ApKHC1 complexes isolated from *Aplysia* CNS and searched for the presence of Calcium/Calmodulin dependent protein kinase IIα (CaMK IIα) mRNA, a transcript reportedly transported by kinesin (14, 17). We used ApC/EBP mRNA, a transcription factor, as a negative control. Semiquantitative RT-PCR experiments showed the presence in the complex of CaMK IIα mRNA and absence of the Aplysia CCAAT/enhancer-binding protein (ApC/EBP) mRNA, suggesting that the complex contains some previously described RNA cargo of kinesin (Fig. 1*D*).

To adopt a genomics approach to identifying all RNAs present in the ApKHC1 complex, we first used *Aplysia* microarrays containing probes corresponding to 56,000 unique neuronal transcripts described previously (18). Fig. 1*E* shows the results of the hybridization analysis carried out on this array showing ~200 RNAs (blue) with at least twofold enrichment in the kinesin complex over control ($P \leq 0.05$) immunoprecipitates from CNS. The RNAs specifically represented in the complex included several neuropeptide precursors, kinases, phosphatases, ion channels, and regulatory factors involved in protein synthesis (Dataset S1, Tables S1, S2, and S3). In this collection, we identified several RNAs that are localized to neuronal processes of sensory neurons, such as elongation factor 1α (19) and sensorin (20–23).

Author contributions: S.V.P. and E.R.K. designed research; S.V.P., I.A., S.K., P.R., Y.-B.C., A.B.K., K.A.K., M.K., and I.M. performed research; S.V.P., I.A., S.K., P.R., Y.-B.C., M.C., F.Y., I.M., and E.R.K. analyzed data; and S.V.P., S.K., J.J.R., J.J., and L.L.M. wrote the paper.

The authors declare no conflict of interest.

Freely available online through the PNAS open access option.

Data deposition: The data reported in this paper have been deposited in the Gene Expression Omnibus (GEO) database, www.ncbi.nlm.nih.gov/geo (accession nos. GSE30440 and GSE30389).

[1]To whom correspondence may be addressed. E-mail: sputhanv@scripps.edu or erk5@columbia.edu.

This article contains supporting information online at www.pnas.org/lookup/suppl/doi:10.1073/pnas.1304422110/-/DCSupplemental.

www.pnas.org/cgi/doi/10.1073/pnas.1304422110

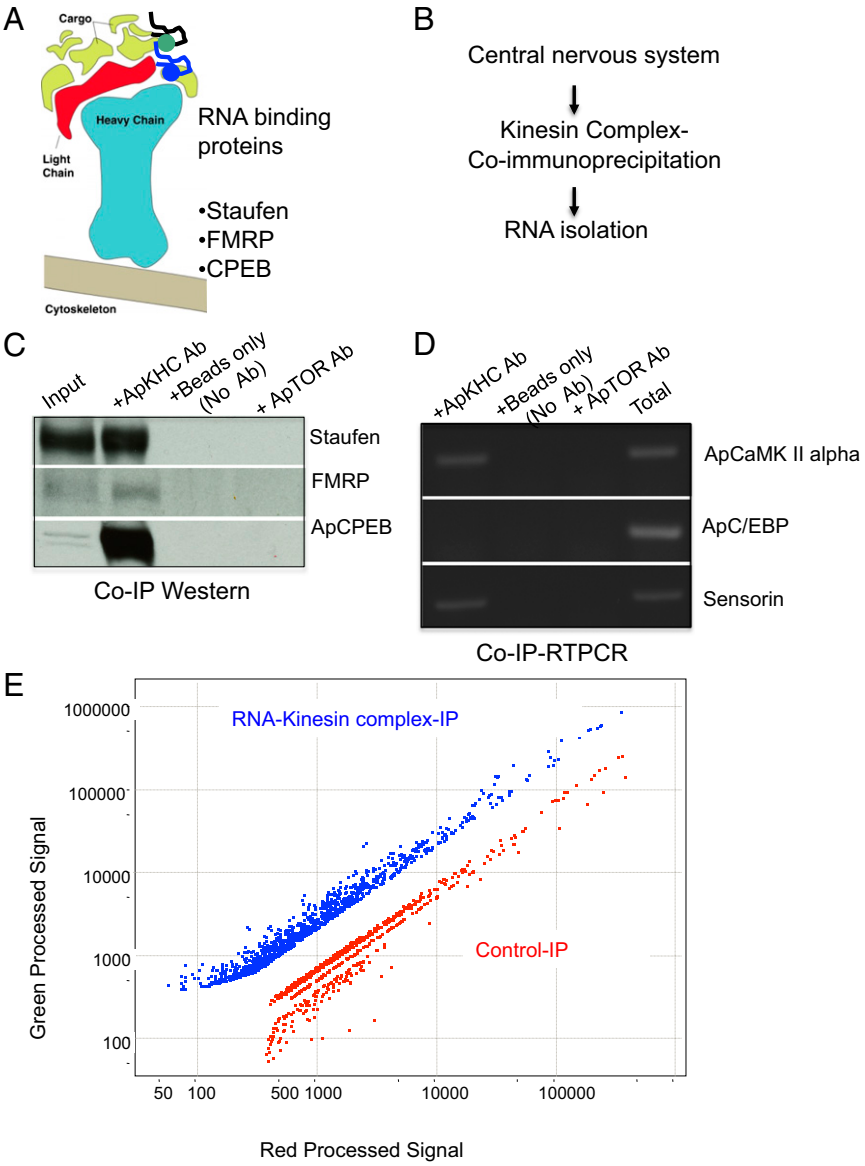

Fig. 1. Isolation and characterization of RNA transport complexes from CNS of *Aplysia*. (*A*) Cartoon representation of RNA transport complex. Components of the transport machinery, including the cytoskeleton, kinesin heavy chain and light chain, and different cargos are shown. Yellow and green irregular shapes represent protein cargos. Dark-blue and green filled circles with squiggly black lines are RNA protein particles (e.g., staufen, FMRP, ApCPEB), which are loaded onto kinesin motors and transported to distal processes. (*B*) Strategy for isolation of transported RNAs. After IP of the kinesin complex from the CNS of *Aplysia*, RNAs were isolated for microarray and RNA-seq studies. (*C*) Western blot analysis of coimmunoprecipitated kinesin complex for the presence of RNA-binding proteins staufen, FMRP, and ApCPEB using specific antibodies. Input, kinesin IP (+ ApKHC Ab), and beads only (no Ab control) are shown. ApTOR Ab was used as a control for IPs. (*D*) qRT-PCR for the presence of positive control CaMK IIα and negative control ApC/EBP transcripts among the RNAs isolated from the kinesin complex. Sensorin mRNA was previously shown to be targeted to sensory neuron processes (21). (*E*) Scatterplot showing RNAs specifically enriched in the kinesin–RNA-binding protein complex (blue) identified by *Aplysia* EST microarray analysis. RNAs isolated from kinesin IPs and control IPs were labeled separately for dual-color microarrays. Data shown correspond to a twofold intensity change after removal of RNAs with $P > 0.01$.

RNA deep sequencing (RNA-seq) Analysis of ApKHC1 Transport Complex Reveals the Complex Composition of Transported RNAs. Our *Aplysia* microarray contained 50–60% of all of the genes predicted to be expressed in the CNS of *Aplysia* (18). An inherent limitation of microarrays is the inability to identify novel and low-abundance transcripts. In addition, the *Aplysia* genome has not yet been fully annotated, and a complete list of *Aplysia* protein-coding genes is not available. Thus, we used the Roche 454 pyrosequencing platform to directly identify all RNAs transported by kinesin. Using 454 sequencing followed by transcript assembly, we identified 5,657 nonredundant sequences (i.e., contigs) of RNAs associated with the kinesin complex prepared from CNS (Dataset S1, Table S4). Approximately 90% of the ~200 RNAs that we identified from the microarray experiments (described above) were found in this collection of RNAs (cf. Dataset S1, Tables S1, S2, S3, and S5), providing independent validation of the microarray results. Therefore, we are reasonably confident that the majority of transcripts identified by RNA-seq indeed comprise a significant portion of the kinesin transport complex. Our RNA-seq analysis has identified ~2,000 transcripts not previously represented in the *Aplysia* EST database.

Using BLAST searches (e-value $<10^{-4}$) in GenBank and SwissProt databases, among the 5,657 identified RNA sequences associated with the CoIP kinesin complex, we were able to identify 1,184 transcripts encoding predicted proteins with known homologs from other organisms (Fig. 2*A* and Dataset S1, Table S5). Based on their predicted physiological functions, these RNAs code for signaling molecules (15.8%), components of the protein synthesis machinery (13.5%), channels and receptors (5.9%), neuropeptides (2.5%), elements of the cytoskeleton (3.9%), components of the protein degradation machinery (1.9%), metabolic and other processes (32.2%), and unknown proteins (24.3%). Importantly, the majority of known *Aplysia* secretory signaling molecules, including neuropeptide precursors and other secretory peptides (e.g., tolloid/bone morphogenetic proteins) (Dataset S1, Table S6) were found in the complex. In comparison, neuropeptide RNAs represent <0.5% of the total transcripts that we recently characterized from the CNS (18) These data suggest that there is substantial enrichment for this class of RNAs in the kinesin complex, and that in general, most neuropeptide RNAs may be transported to the synapses.

Consistent with previous findings on mRNA localization in the sensory neuron processes (18, 21), we identified transcripts encoding nearly all of the ribosomal proteins and the majority of components of the protein synthesis machinery and RNA-binding proteins, such as staufen and zinc finger dsRNA-binding proteins,

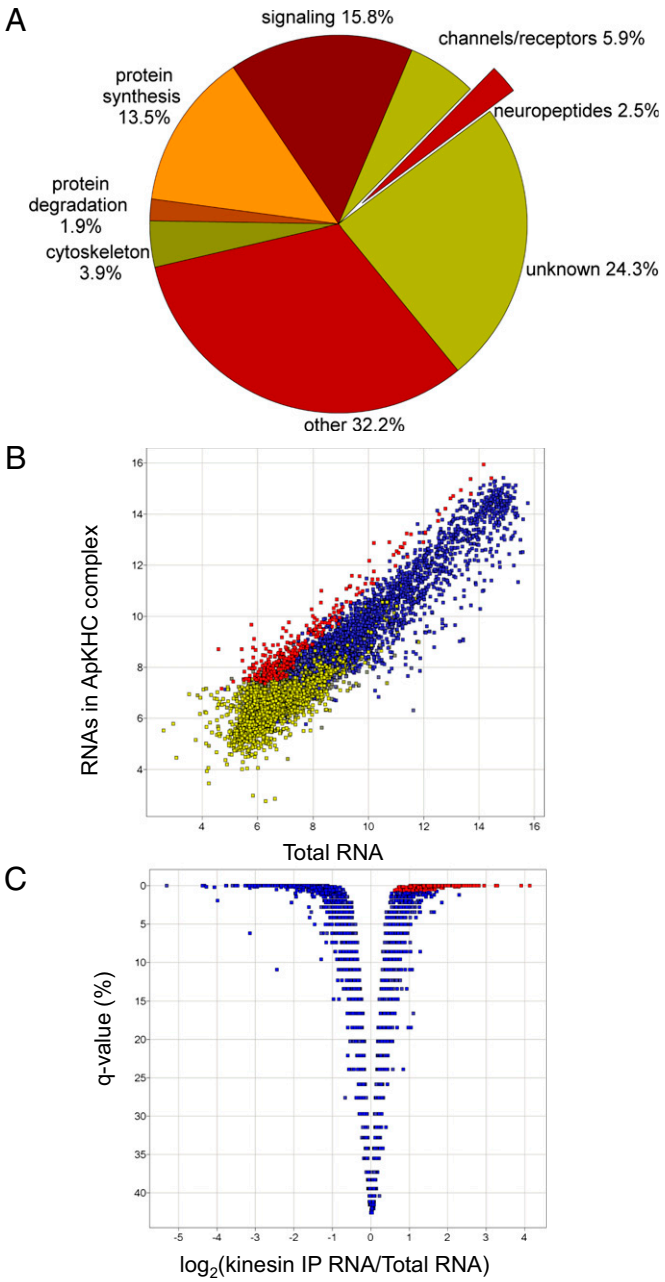

Fig. 2. Genomic characterization of the kinesin transport complex. (*A*) Pie chart showing different functional groups of gene products identified from RNA-seq analysis of RNAs prepared from the kinesin complex coimmunoprecipitated from CNS. (*B* and *C*) Characterization of kinesin-transported RNAs using cargo-enriched microarrays. Scatterplot of normalized signal intensities of kinesin IP and total RNA microarrays (*B*), and *q*-value vs. enrichment ratio diagram (*C*) of kinesin IP-enriched fraction detected by microarrays. The color code is the same in both diagrams. The 317 transcripts shown in red in both diagrams have statistically significant enrichment in kinesin IP at a median FDR of <0.62% compared with the total RNAs from CNS. Transcripts that were not detected on both kinesin IP and total RNA microarrays in at least three experiments (shown in yellow) were removed from further analysis. Transcripts that did not show significant enrichment in kinesin IP with respect to total RNAs are shown in blue.

as well as components of the cytoskeleton, and cytoskeleton-associated regulatory proteins, including myosin, tubulin, actin, and kinesin-like protein (Table S5). Also present in the complex were components of signal transduction pathways, including kinases (e.g., protein kinase A, C, G), phosphatases, lipases, calmodulin, ion channels (e.g., hyperpolarization-activated ion channel, Phe-Met-Arg-Phe-NH2 (FMRFamide)-gated Na^+ channel), neurotransmitter transporters (e.g., vesicular acetylcholine transporter), synaptic proteins (e.g., synaptotagmin-1, synaptobrevin, NMDA-type glutamate, other receptors, including seven transmembrane helix receptors), and cell adhesion molecules (e.g., neural cell adhesion molecule [NCAM]-related adhesion molecule). We also discovered several natural antisense/non-coding RNAs (e.g., natural antisense RNAs for beta tubulin, S6 kinase, protein kinase A type II) in the complex (Fig. S1), suggesting that they also might be transported and contribute to synaptic physiology and memory storage. We next compared recently published data on RNA localization in rat hippocampal neurons with that of our current dataset on kinesin-associated RNAs identified from *Aplysia* CNS. Bioinformatics analysis suggest that they share ~40% Gene Ontology terms (Fig. S2 and Dataset S1, Table S10), suggesting a major overlap of signaling pathways present in hippocampal and *Aplysia* CNS neuronal processes.

RNA Cargo-Enriched Microarray Analysis Suggests Enrichment of Specific RNAs in the ApKHC1 Complex from *Aplysia* CNS. To determine whether there is a substantial enrichment of certain RNAs in the transport complex, we compared gene expression profiles of total RNAs expressed in the CNS and RNAs present in the ApKHC1 complex using *Aplysia* microarrays (18) supplemented with the ~2,000 additional gene probes identified by 454 sequencing. We then used this kinesin cargo-enriched array to compare RNAs present in the immunoprecipitated complex from CNS and total RNA from CNS.

Our microarray results suggest a significant enrichment of many RNAs in the kinesin immunoprecipitates, supporting our initial characterization (Fig. 2 *B* and *C* and Fig. S3). The enrichment of 317 transcripts in the kinesin immunoprecipitation (IP) complex (shown in red in Fig. 2 *B* and *C*) was statistically significant, with a median false discovery rate (FDR) <0.62%, which would correspond to approximately two false-positive results in the set. The functional assignment was based on homology searches and information obtained from EST sequencing. These transcripts in the kinesin IP complex included homologs for ash1 (asymmetric synthesis of HO endonuclease1), SFRS8 (splicing factor, arginine/serine-rich 8), cyclin-dependent kinase activator, cactin, and heat shock protein 60 (HSP60) (Dataset S1, Table S7). Of note, 40% of the transcripts that we identified as enriched in the kinesin complex compared with the total RNA were among the 2,000 additional features that we added to make the cargo-enriched array, thereby further validating our initial microarray and RNA-seq results.

We next studied the 317 transcripts identified as enriched in the ApKHC1 complex to identify biological pathways possibly mediated by these RNA cargos. Because *Aplysia* currently does not have a complete well-annotated genome and transcriptome, we identified human homologs of the *Aplysia* ESTs using *blastx* searches against the human transcriptome. Out of 317 cargo-enriched transcripts (significant at 1% FDR), 147 transcripts produced hits in the human transcriptome (Dataset S1, Table S8). We further analyzed these 147 transcripts using the Expression Analysis Systematic Explorer (EASE) (30) to search for predominant biological themes in gene annotation databases and the Kyoto Encyclopedia of Genes and Genomes (KEGG) using *Aplysia* array projection into the human transcriptome, as a background for statistical estimations (Dataset S1, Table S9). From this analysis, we identified 16 homologous pathways, including pathways involved in basic cellular processes, such as protein export, calcium signaling, axon guidance, endocytosis, cytoskeletal regulation, and RNA splicing, and diseases, such as Huntington's disease. Not surprisingly, our findings suggest that RNAs transported by kinesin could regulate several different physiological processes at the CNS synapses.

Myosin Heavy Chain, an RNA Cargo of Kinesin, Is Required for the Establishment of LTF. We next localized three candidate RNA cargos of ApKHC1 by RNA in situ hybridization, using a hybridization

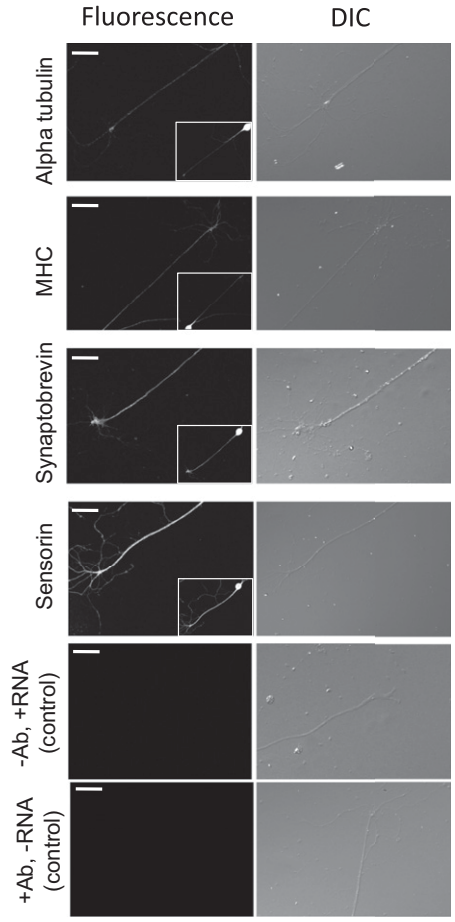

Fig. 3. In situ hybridization analysis of cargo candidates. Three different cargos (ApMHC, α-tubulin, and synaptobrevin) were analyzed by in situ hybridization of sensory neurons using digoxigenin-labeled riboprobes. After hybridization and washing, these RNAs were visualized using a fluorescent tyramide detection system. Confocal projection images of sensory neuron processes and corresponding differential interference contrast (DIC) are shown. (*Insets*) Projection images of the whole neurons. Localization of sensorin RNA served as a positive control. The specificity controls for in situ hybridization consisted of the Ab but no labeled RNA probes and labeled RNA probes but no Ab. (Scale bar: 50 μm.)

probe for sensorin as a positive control. We found that synaptobrevin, α-tubulin, and myosin heavy chain (MHC) RNAs localized to sensory neuron processes (Fig. 3). α-tubulin has previously been found to be localized to sensory neurons (18, 21), which is of interest in understanding molecular motor-dependent transport and localization of proteins and RNAs to distal neuronal processes. MHCs are actin-dependent molecular motors critical for hippocampal long-term potentiation (LTP) (24, 25).

We first examined whether knockdown of ApKHC1 would affect the localization of *Aplysia* MHC (ApMHC). We injected ApKHC1 antisense oligonucleotides (15) into sensory neurons to disrupt kinesin-mediated transport and examined localization of MHC RNAs at the processes by in situ hybridization analysis. Analysis of the confocal projection images showed a ~30% decrease in ApMHC staining [unpaired t test, two-tailed P value = 0.014; $t(7) = 3.28$; mean fluorescence intensity ± SEM of ApMHC staining: control, 21.7 ± 2.03, (n = 4); ApKHC knockdown, 15.1 ± 0.78 (n = 5)] in the processes of sensory neurons that received ApKHC1 antisense oligonucleotide injection (Fig. 4 *A* and *B*).

We next examined whether repeated exposure to serotonin (5HT), a modulatory neurotransmitter that produces LTF at sensory and motor neuron synapses, regulates the expression of ApMHC RNA in sensory neurons. Quantitative RT-PCR (qRT-PCR) showed that exposure to five pulses of 5HT (5× 5HT) increased ApMHC RNA levels in sensory neuron clusters (normalized fold increase after 1 h of 5HT exposure, 1.8 ± 0.13; after 6 h of exposure, 0.93 ± 0.37; n = 6; Student t test) (Fig. 5*A*). Expression of ApC/EBP was used as a positive control for 5× 5HT treatment.

To explore the significance of ApMHC up-regulation during memory storage, we studied the electrophysiological consequences of specific knockdown of ApMHC in sensory neurons during short-term facilitation (STF) and initiation and persistence of LTF of sensory and motor neuron synapses. We injected antisense oligonucleotides that specifically degrade ApMHC [unpaired t test, two-tailed P values: control vs antisense-injected, P = 0.0031, t (10) = 3.87; sense oligonucleotide vs antisense-injected, P = 0.0005, t (10) = 5.11; mean fluorescence intensity ± SEM of ApMHC staining: control, 19.5 ± 1.73 (n = 6); sense oligonucleotide, 20.8 ± 1.48 (n = 6); antisense oligonucleotide, 12.1 ± 0.84 (n = 6)] into sensory neurons and measured excitatory post synaptic potentials (EPSPs) (Fig. 4 *C* and *D*).

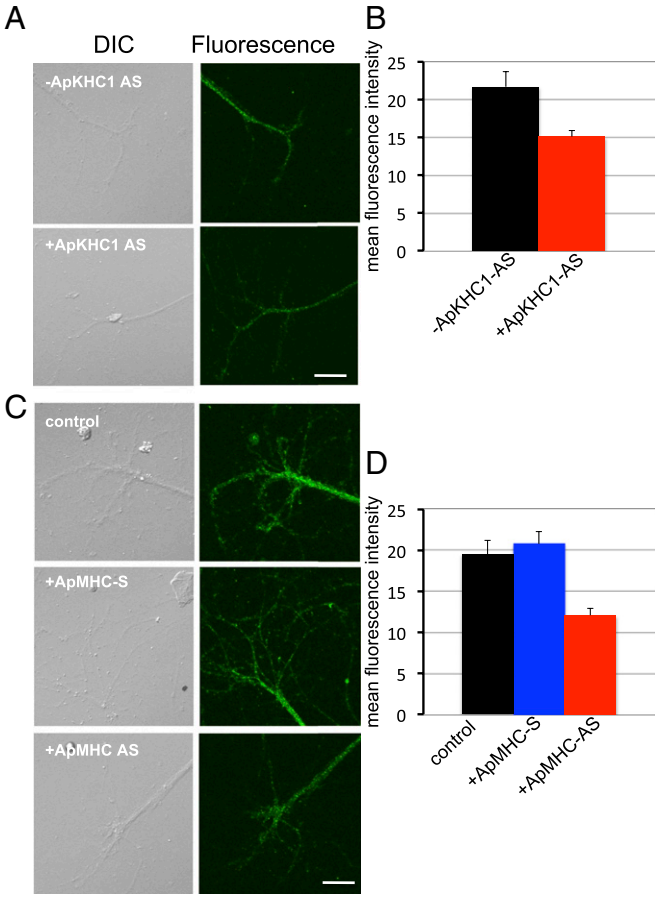

Fig. 4. Characterization of ApMHC localization at sensory neuron processes. (*A*) Confocal projection image showing ApMHC RNA staining using fluorescent antisense riboprobes in sensory neuron processes. Antisense oligonucleotides against ApKHC1 (ApKHC1 AS) were injected into sensory neurons. (*B*) Quantitation of in situ hybridization data (uninjected controls, n = 4; ApKHC1 AS injected, n = 5) shown in *A*. The images were analyzed using MetaMorph (Molecular Devices); mean fluorescence intensities are shown (P < 0.05, two-tailed unpaired t test). Error bars represent SEM. (*C*) Confocal projection image showing ApMHC RNA staining using fluorescent antisense riboprobes in sensory neuron processes. ApMHC AS, antisense oligonucleotides against ApMHC; ApMHC S, sense oligonucleotides against ApMHC. (*D*) Quantitation of in situ hybridization data (uninjected, n = 6; ApMHC S oligonucleotide injected, n = 6; ApMHC AS oligonucleotide injected, n = 6) shown in *C*. The images were analyzed using MetaMorph; mean fluorescence intensities are shown (P < 0.05, two-tailed unpaired t test). Error bars are SEM. Scale bar: 50 μm.

We began by examining STF. For this, ApMHC oligonucleotides (sense and antisense) were injected into sensory neurons cocultured with L7 motor neurons (31). At 4 h after oligonucleotide injection, the cultures were treated with 10 μM 5HT for 5 min. EPSPs were recorded (Fig. 5*B*) after 10 min of 5HT treatment. An uninjected sensory neuron synapsing with the same motor neuron was used as an internal control for injection. We found the following percent changes in mean EPSP amplitudes: control (untreated), −10.3 ± 7.9 (n = 7); antisense MHC oligonucleotide alone: 7.5 ± 6.4 (n = 10); sense MHC oligonucleotide alone, 1.9 ± 6.1 (n = 6); one pulse of 5HT (1× 5HT), 139.14 ± 51.5 (n = 7); antisense MHC + 1× 5HT, 137.2 ± 27.4 (n = 10); sense MHC + 1× 5HT, 143 ± 25.1 (n = 12). Our data shows that neurons that were exposed to single pulses of 5HT, 5HT + antisense ApMHC, and 5HT + sense ApMHC showed no statistically significant differences in EPSPs (F = 0.1924; P = 0.8264, repeated-measures ANOVA; $P > 0.05$, Tukey's multiple-comparison test), suggesting that ApMHC RNA levels are not critical for STF.

To determine the role of ApMHC in LTF, we next injected antisense and sense oligonucleotides into sensory neurons in the coculture and then applied five pulses of 10 μM 5HT at 4 h after oligonucleotide injection. Measurements of EPSPs at 24 h and 48 h after the 5HT exposure revealed the following percent changes in mean EPSP amplitudes: 5HT alone: at 24 h, +57 ± 7.5 (n = 8); at 48 h, +51.4 ± 6.7 (n = 8); 5HT + ApMHC antisense oligonucleotide: at 24 h, +3.14 ± 8.5 (n = 12); at 48 h, +3.9 ± 11 (n = 12); 5HT + ApMHC sense oligonucleotide: at 24 h, + 52.9 ± 14.7 (n = 8); at 48 h, +46 ± 10.7 (n = 8) (Fig. 5*C*). Neither the antisense nor the sense MHC oligonucleotides affected basal synaptic transmission. However, the antisense oligonucleotides blocked the 5HT-dependent increase in EPSPs [$F(8, 88)$ = 4.3825; P = 0.00017, repeated-measures ANOVA; $P < 0.001$, Newman–Keuls post hoc test at both 24 h and 48 h], suggesting that ApMHC is required for the establishment of LTF (Fig. 5*C*).

We then asked whether inhibition of MHC would affect the persistence of LTF. We injected MHC antisense oligonucleotides at 24 h after induction of LTF with exposure to 5HT and measured EPSPs at 48 h. Interestingly, we found that MHC inhibition did not affect the persistence of LTF. Percent changes in EPSP amplitudes measured at 48 h after exposure to 5HT alone and to 5HT + antisense oligonucleotide injected at 24 h were not significantly different [5HT + ApMHC antisense oligonucleotide injected at 24 h, +73 ± 17.3 (n = 9); at 48 h, +58 ± 11 (n = 9); t (11) = 0.04; two-tailed P value = 0.9722, unpaired t test] (Fig. 5*C*). These results suggest that ApMHC levels are important for the initiation of LTF, but not for persistence of LTF at *Aplysia* sensory and motor neuron synapses.

Discussion

Characterization of ApKHC1 Transport Complex Has Led to Identification of RNAs Actively Targeted to Synapses of *Aplysia* CNS. Several previous studies that characterized RNAs prepared from dissected processes of cultured neurons have identified distally localized RNAs in neurons (2, 18, 21, 26). The methodologies applied in those studies are not useful for directly identifying RNAs targeted to synapses of intact brain or brain regions, however. Our NextGen sequence analysis of RNAs isolated from kinesin immunoprecipitates allowed us to identify approximately 5,657 transcripts from *Aplysia* CNS, 1,184 of which were annotated using Gene Ontology terminology. This analysis will improve as the availability of *Aplysia* genome sequence and gene annotation increases. The RNAs identified in the kinesin complex constitute ~2–5% of the predicted transcriptome of the *Aplysia* genome. We also identified several naturally occurring antisense RNA transcripts with functions at synapses that remain to be determined. Our analyses suggest that the transported RNAs are surprisingly diverse and pose the question of why so many different RNAs are targeted to synapses.

One possible explanation is that these different mRNAs are stored at the synapses for later use. Translation of these RNAs might be regulated at specific synapses during the process of storing, maintaining, and reconsolidating long-term memories not only for modifying preexisting synaptic connections, but also for the

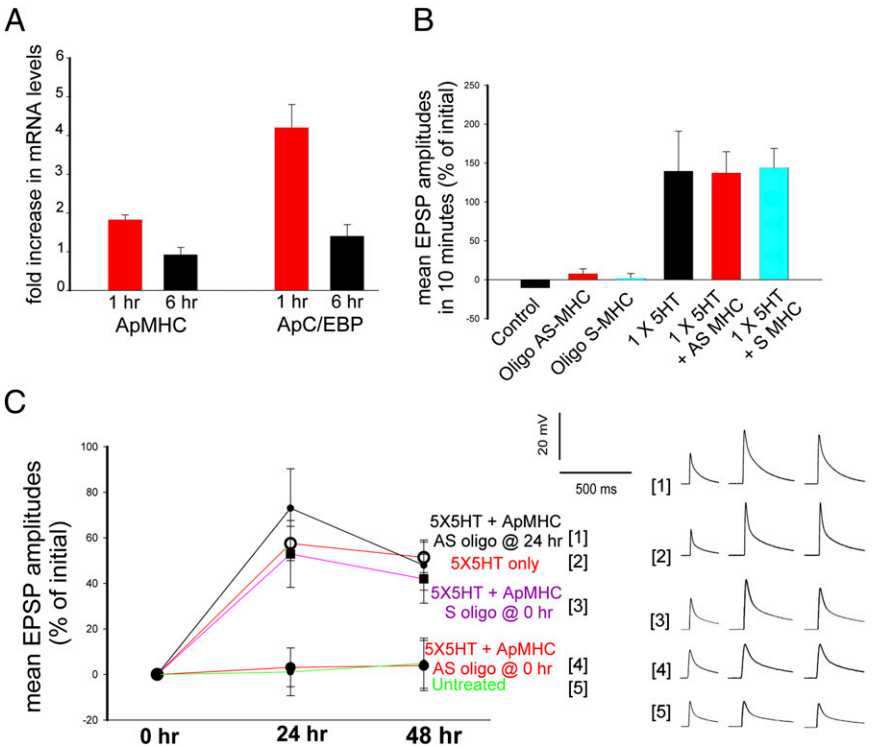

Fig. 5. MHC, an RNA cargo of kinesin, is required for establishment of LTF. (*A*) Transcriptional regulation of ApMHC by 5 pulses of 5HT (5× 5HT). RNAs were extracted from sensory neuron clusters 1 h (red bars) or 6 h (black bars) after 5× 5HT treatment. ApC/EBP was used as positive control for 5HT application. Data were normalized to ApGAPDH levels. (n = 4, $P < 0.05$, Student's t test. Error bars are SEM); *B* and C: Electrophysiological characterization of MHC function in different phases of memory storage. (*B*) STF measurements. Antisense (AS) and sense (S) oligonucleotides were injected into sensory neurons. After 4 h of injection, neurons were treated with 1× 10 M 5HT and EPSPs were recorded after 10 min. Changes in EPSPs levels were quantified and presented as mean SEM. control (n = 7); antisense MHC oligo alone (n = 10); sense MHC oligo alone (n = 6); 1× 5HT (n = 7); antisense MHC + 1× 5HT (n = 10); sense MHC + 1× 5HT (n = 12). Inhibition of MHC RNA did not affect STF ($P > 0.05$, ANOVA and Tukey's multiple comparison test); (*C*) LTF measurements. After 4 h of AS and S MHC oligonucleotide injection, neurons were exposed to 5× 10 M 5HT and EPSPs were recorded at 24 and 48 h after 5HT exposure. To determine effect of knockdown during persistence, AS oligonucleotides were injected at 24 h after the 5HT treatment, and EPSPs were recorded after 48 h of initial 5HT exposure. MHC knockdown blocked the initiation phase ($P <$ 0.05, ANOVA and Newman-Keuls post hoc test). 5HT alone: at 24 h, n = 8; at 48 h, n = 8; 5HT + ApMHC AS oligo: at 24 h, n = 12; at 48 h, n = 12; 5HT + ApMHC Sense oligo: at 24 h, n = 8; at 48 h, n = 8. However, once the LTF is induced, blocking of MHC by antisense oligonucleotides does not have any statistically significant ($P > 0.5$, unpaired two-tailed t test) effect on persistence. 5HT + ApMHC oligo AS injected at 24 h, n = 9; at 48 h, n = 9. Sense or antisense oligos by themselves did not affect basal transmission. Error bars are SEM.

formation of new ones. Consistent with this idea, Si et al. (27, 28) have demonstrated learning-dependent activation of synaptically localized RNAs by polyadenylation, which is mediated by CPEB.

Role of Active Molecular Transport in Initiation and Persistence of Long-Term Memories. We previously found that microtubule-dependent kinesin motors are essential for the initiation of LTF, but not for its persistence (15). This finding led us to consider the possibility that during the persistence phase, actin/MHC-dependent delivery of cargos might be important. Contrary to our expectation, however, we found that MHC antisense oligonucleotides blocked initiation of LTF, but did not affect persistence of LTF when injected into sensory neurons at 24 h after initiation. These results suggest that MHC levels are no longer critical during the persistence phase. Consistent with the requirement of ApMHC for the initiation of LTF, MHC has been found to be critical for LTP of the CA1 region of mouse hippocampus (24, 25). Taken together, our results lead us to conclude that during the early initiation phase of memory storage, the neuron uses active transport mechanisms, such as microtubule and actin-dependent motors, for delivery of cargos to synapses, but that once gene products arrive at their destination, enhanced microtubule- and actin-dependent delivery of molecules is no longer necessary for the persistence of memory storage. At this point, other mechanisms, including basal levels of transport, local regulation of translation, and local protein synthesis, become key determinants of persistence. Thus, these motors control the late phases of plasticity indirectly by supplying the population of mRNAs and proteins that are required for maintenance.

Experimental Procedures

Details of 5HT stimulation, isolation of proteins and RNAs, cloning, antibodies, oligonucleotides, qRT-PCR, Western blot analysis, in situ hybridization, microinjection, and electrophysiology are provided in *SI Experimental Procedures*.

IP of Kinesin Complex and RNA Isolation. We modified previously described buffer conditions to isolate kinesin complexes from the *Aplysia* CNS (15). The modified buffer contained 50 mM Tris·HCl (pH 7.5), 150 mM NaCl, 1 mM EDTA, 1 mM KCl, 0.5% Nonidet P-40, 1 mM DTT, 1% ultrapure BSA (Ambion), 1% yeast tRNA, and inhibitors of proteases (Roche), phosphatases (Sigma-Aldrich), and RNAses (Ambion). All of the experiments were conducted at 4 °C in an RNAse-free environment. Precleared extracts prepared from two adult (50–90 g) *Aplysia* CNS (for one IP experiment, $n = 1$) were incubated with 20 μg of affinity-purified anti-kinesin Ab (15). After 6 h of incubation on a rotator, protein A/G beads (Pierce) were added to the immunoprecipitates, followed by another 1 h of rotation. The immunoprecipitates were washed three times using the same buffer, followed by brief centrifugation (100 × g for 2 min). These washes were carried out in separate Eppendorf tubes (siliconized Rnase-free) to minimize nonspecific binding of RNA to the plastic. After the third wash, the beads were incubated with Trizol to prepare RNA for Agilent Bioanalyzer, 454 sequencing, microarrays, and qRT-PCR analyses. Equivalent amounts of a rabbit polyclonal Ab against ApTOR protein was used in control IPs.

cDNA Library Construction for 454 Sequencing. We used commercial kits (Marathon cDNA Amplification Kit, catalog no. 634913; Clontech) to ensure consistency and reproducibility of library preparations. Methods used for 454 library construction and sequencing have been described previously (29). Three independent biological replicates were sequenced. All original sequence reads were submitted to the National Center for Biotechnology Information's Sequence Read Archive (project no. SRA009823.3). A total of 40,204 reads were generated, assembled, and used for analysis. The Velvet assembly (32) generated 5,657 unique transcripts.

Microarray Analysis. Microarray and sample preparation and hybridization were performed as described previously (18, 29). Custom microarrays supplemented with 2,000 additional features containing probes (Agilent) for kinesin-immunoprecipitated transcripts identified by 454 sequencing were used in later experiments.

ACKNOWLEDGMENTS. We thank Kaben Schwartz for the initial characterization of cargo RNAs by qRT-PCR and preparation of probes for in situ hybridization, and Vivian Zhu and Eddy Konstantinov for preparation of *Aplysia* neuronal cultures. This work was supported by the Howard Hughes Medical Institute, National Institutes of Health (Grants P50 HG002806, MH075026, 1R01 NS060762, 1R01 GM097502, R21RR025699, and 5R21DA030118), McKnight Brain Research Foundation, Whitehall Foundation, and National Science Foundation (Grant 0744649).

1. Bailey CH, Kandel ER, Si KS (2004) The persistence of long-term memory: A molecular approach to self-sustaining changes in learning-induced synaptic growth. *Neuron* 44(1):49–57.
2. Cajigas IJ, et al. (2012) The local transcriptome in the synaptic neuropil revealed by deep sequencing and high-resolution imaging. *Neuron* 74(3):453–466.
3. Frey U, Krug M, Reymann KG, Matthies H (1988) Anisomycin, an inhibitor of protein synthesis, blocks late phases of LTP phenomena in the hippocampal CA1 region in vitro. *Brain Res* 452(1-2):57–65.
4. Huang YY, Nguyen PV, Abel T, Kandel ER (1996) Long-lasting forms of synaptic potentiation in the mammalian hippocampus. *Learn Mem* 3(2-3):74–85.
5. Kandel ER (2001) The molecular biology of memory storage: A dialogue between genes and synapses. *Science* 294(5544):1030–1038.
6. Kiebler MA, DesGroseillers L (2000) Molecular insights into mRNA transport and local translation in the mammalian nervous system. *Neuron* 25(1):19–28.
7. Krug M, Lössner B, Ott T (1984) Anisomycin blocks the late phase of long-term potentiation in the dentate gyrus of freely moving rats. *Brain Res Bull* 13(1):39–42.
8. Martin KC, et al. (1997) Synapse-specific, long-term facilitation of *Aplysia* sensory to motor synapses: A function for local protein synthesis in memory storage. *Cell* 91(7):927–938.
9. McGuire SE, Deshazer M, Davis RL (2005) Thirty years of olfactory learning and memory research in *Drosophila melanogaster*. *Prog Neurobiol* 76(5):328–347.
10. Miniaci MC, et al. (2008) Sustained CPEB-dependent local protein synthesis is required to stabilize synaptic growth for persistence of long-term facilitation in *Aplysia*. *Neuron* 59(6):1024–1036.
11. Stanton PK, Sarvey JM (1984) Blockade of long-term potentiation in rat hippocampal CA1 region by inhibitors of protein synthesis. *J Neurosci* 4(12):3080–3088.
12. Tully T, Preat T, Boynton SC, Del Vecchio M (1994) Genetic dissection of consolidated memory in *Drosophila*. *Cell* 79(1):35–47.
13. Hirokawa N (1998) Kinesin and dynein superfamily proteins and the mechanism of organelle transport. *Science* 279(5350):519–526.
14. Kanai Y, Dohmae N, Hirokawa N (2004) Kinesin transports RNA: Isolation and characterization of an RNA-transporting granule. *Neuron* 43(4):513–525.
15. Puthanveettil SV, et al. (2008) A new component in synaptic plasticity: Up-regulation of kinesin in the neurons of the gill-withdrawal reflex. *Cell* 135(5):960–973.
16. Tübing F, et al. (2010) Dendritically localized transcripts are sorted into distinct ribonucleoprotein particles that display fast directional motility along dendrites of hippocampal neurons. *J Neurosci* 30(11):4160–4170.
17. Rook MS, Lu M, Kosik KS (2000) CaMKIIalpha 3′ untranslated region-directed mRNA translocation in living neurons: Visualization by GFP linkage. *J Neurosci* 20(17):6385–6393.
18. Moroz LL, et al. (2006) Neuronal transcriptome of *Aplysia*: Neuronal compartments and circuitry. *Cell* 127(7):1453–1467.
19. Giustetto M, et al. (2003) Axonal transport of eukaryotic translation elongation factor 1α mRNA couples transcription in the nucleus to long-term facilitation at the synapse. *Proc Natl Acad Sci USA* 100(23):13680–13685.
20. Brunet JF, Shapiro E, Foster SA, Kandel ER, Iino Y (1991) Identification of a peptide specific for *Aplysia* sensory neurons by PCR-based differential screening. *Science* 252(5007):856–859.
21. Moccia R, et al. (2003) An unbiased cDNA library prepared from isolated *Aplysia* sensory neuron processes is enriched for cytoskeletal and translational mRNAs. *J Neurosci* 23(28):9409–9417.
22. Schacher S, Wu F, Panyko JD, Sun ZY, Wang DN (1999) Expression and branch-specific export of mRNA are regulated by synapse formation and interaction with specific postsynaptic targets. *J Neurosci* 19(15):6338–6347.
23. Wang DO, et al. (2009) Synapse- and stimulus-specific local translation during long-term neuronal plasticity. *Science* 324(5934):1536–1540.
24. Rex CS, et al. (2010) Myosin IIb regulates actin dynamics during synaptic plasticity and memory formation. *Neuron* 67(4):603–617.
25. Wang ZP, et al. (2008) Myosin Vb mobilizes recycling endosomes and AMPA receptors for postsynaptic plasticity. *Cell* 135(3):535–548.
26. Poon MM, Choi SH, Jamieson CAM, Geschwind DH, Martin KC (2006) Identification of process-localized mRNAs from cultured rodent hippocampal neurons. *J Neurosci* 26(51):13390–13399.
27. Si K, Choi YB, White-Grindley E, Majumdar A, Kandel ER (2010) *Aplysia* CPEB can form prion-like multimers in sensory neurons that contribute to long-term facilitation. *Cell* 140(3):421–435.
28. Si K, et al. (2003) A neuronal isoform of CPEB regulates local protein synthesis and stabilizes synapse-specific long-term facilitation in aplysia. *Cell* 115(7):893–904.
29. Moroz LL, Kohn AB (2010) Do different neurons age differently? Direct genome-wide analysis of aging in single identified cholinergic neurons. *Front Aging Neurosci* 2:1–18.
30. Dennis et al. (2003) DAVID: Database for Annotation, Visualization, and Integrated Discovery. *Genome Biol* 4(5):P3.
31. Montarolo PG et al. (1986) A critical period for macromolecular synthesis in long-term heterosynaptic facilitation in Aplysia. *Science* 234(4781):1249–1254.
32. Zerbino DR, Birney E (2008) Velvet: algorithms for de novo short read assembly using de Bruijn graphs. *Genome Res* 18(5):821–829.